

¹⁶M. M. Abraham, C. B. Finch, L. J. Raubenheimer, Z. M. el Saffar, and R. A. Weeks, in *Proceedings of the Fourteenth Colloque Ampère: Magnetic Resonance and Relaxation, Ljubljana*, 1966 (North-Holland, Amsterdam, 1967), p. 282.

¹⁷See, for example, M. M. Abraham, L. A. Boatner, C. B. Finch, E. J. Lee, and R. A. Weeks, *J. Phys. Chem. Solids* **28**, 81 (1967).

¹⁸J. Ranon and J. S. Hyde, *Phys. Rev.* **141**, 259 (1966).

¹⁹D. Descamps and Y. Merle d'Aubigne, *Phys. Letters* **8**, 5 (1964).

²⁰I. C. Chang and W. W. Anderson, *Phys. Letters* **13**, 112 (1964).

²¹M. M. Abraham and L. A. Boatner, *J. Chem. Phys.* **51**, 3134 (1969).

²²J. Ranon and W. Low, *Phys. Rev.* **132**, 1609 (1963).

²³M. M. Abraham, R. A. Weeks, G. W. Clark, and C. B. Finch, *Phys. Rev.* **137**, A138 (1965).

²⁴M. M. Abraham, R. A. Weeks, G. W. Clark, and C. B. Finch, *Phys. Rev.* **148**, 350 (1966).

²⁵H. R. Lewis and E. S. Sabisky, *Phys. Rev.* **130**, 1370 (1963).

²⁶A. Abragam and B. Bleaney, *Electron Paramagnetic Resonance of Transition Ions* (Clarendon, Oxford, England, 1970), p. 730.

PHYSICAL REVIEW B

VOLUME 3, NUMBER 9

1 MAY 1971

Electron-Paramagnetic-Resonance Investigations of $5f^5$ Configuration Ions in Cubic Single Crystals: Pu^{3+} in ThO_2 and SrCl_2 , and Am^{4+} in ThO_2 [†]

M. M. Abraham, L. A. Boatner,* C. B. Finch,[‡] and R. W. Reynolds*

Solid State Division, Oak Ridge National Laboratory, Oak Ridge, Tennessee 37830

(Received 18 December 1970)

Electron-paramagnetic-resonance spectra of the isoelectronic ions Pu^{3+} and Am^{4+} in cubic sites of fluorite-structure single crystals have been investigated at 1.5 and 4.2 K. The observed isotropic spectra and associated g values identify the ground states as Γ_7 doublets. This ground state is produced by intermediate-coupling effects which are much larger for $5f^5$ configuration ions than for the analogous $4f^5$ ions. Spin-Hamiltonian parameters were determined to be: $g=1.3124\pm 0.0005$, $A=(65.4\pm 0.2)\times 10^{-4}\text{ cm}^{-1}$ for $^{239}\text{Pu}^{3+}$ in ThO_2 ; $g=1.1208\pm 0.0005$, $A=(127.9\pm 0.4)\times 10^{-4}\text{ cm}^{-1}$ for $^{239}\text{Pu}^{3+}$ in SrCl_2 ; and $g=1.2862\pm 0.0005$, $A=(45.7\pm 0.1)\times 10^{-4}\text{ cm}^{-1}$ for $^{241}\text{Am}^{4+}$ and $A=(45.3\pm 0.1)\times 10^{-4}\text{ cm}^{-1}$ for $^{243}\text{Am}^{4+}$ in ThO_2 . Spectra observed for both Pu^{3+} and Am^{4+} were characterized by very anisotropic linewidths and by a dependence of linewidth on the nuclear-spin projection quantum number m_I .

I. INTRODUCTION

Although the electronic properties of $5f^n$ (actinide) ions are somewhat similar to those of the corresponding $4f^n$ (rare-earth) ions, some important differences occur as a result of intermediate-coupling effects. An illustration of the significance of intermediate coupling for the actinide ions was provided by a comparison¹ of wave functions calculated for the $J=\frac{5}{2}$ ground-state term of Sm^{3+} ($4f^5$) and Pu^{3+} ($5f^5$). For pure Russell-Saunders coupling, the Hund's-rule ground state for an f^5 configuration is ${}^6H_{5/2}$. A comparison of the intermediate-coupled wave functions, however, indicated that although the 6H term contributes 96% to the ground state of Sm^{3+} , it contributes only 66% to the Pu^{3+} ground state.

The large admixture of higher-lying $J=\frac{5}{2}$ states changes the predicted splitting by a cubic crystal field of the Pu^{3+} ground-state term. A calculation of the fourth-order crystal-field operator-equivalent factors $\langle \Psi_J || \beta || \Psi_J \rangle$ has been carried out by Edelstein *et al.*¹ using intermediate-coupled wave functions for Sm^{3+} and Pu^{3+} . From this calculation they found that intermediate coupling resulted in a differ-

ence in the sign of the factor $\langle \Psi_J || \beta || \Psi_J \rangle$ for Pu^{3+} relative to that obtained for Sm^{3+} (or for a pure ${}^6H_{5/2}$ state). For Sm^{3+} and Pu^{3+} in an eightfold-coordinated cubic site, this difference in sign determines that the Γ_8 quartet lies lowest for Sm^{3+} , while the Γ_7 doublet lies lowest for Pu^{3+} . Experimentally, Edelstein *et al.*¹ have verified that the Γ_7 doublet is the ground state for Pu^{3+} in CaF_2 , SrF_2 , and BaF_2 . Their measured g values for Pu^{3+} were different in each host due to varying crystal-field-produced admixtures of the Γ_7 doublet in the first excited $J=\frac{7}{2}$ state. A Γ_8 ground state for Sm^{3+} in an eightfold-coordinated cubic site has not been reported, although axial spectra have been observed^{2,3} in CaF_2 .

An interpretation of the Pu^{3+} hyperfine parameters as measured in three fluorite-structure hosts has been given recently by Edelstein and Mehlhorn.⁴ Intermediate-coupling effects were again important, and the varying admixture of the excited Γ_7 doublet also resulted in significant variations in the magnitude of the hyperfine parameter which corresponded to observed effects.

We report here the observation of Pu^{3+} EPR spectra in the fluorite-structure single crystals ThO_2

and SrCl_2 . These materials are particularly interesting hosts, since, based on previous experimental results,⁵ the crystal-field interaction in ThO_2 should be significantly larger than that of the alkaline-earth fluorides, while the SrCl_2 crystal-field strength should be considerably smaller. The observed hyperfine and Zeeman splitting parameters for Pu^{3+} in these hosts, therefore, offer an extended test of the interpretations of Edelstein *et al.*¹ We have also observed the EPR spectrum of tetravalent americium in thorium dioxide. This represents the first reported EPR observation of Am^{4+} in any host crystal.

II. EXPERIMENTAL

Single crystals of thorium dioxide doped with either $^{239}\text{Pu}^{3+}$, $^{241}\text{Am}^{4+}$, or $^{243}\text{Am}^{4+}$ were grown by a thermal-gradient technique⁶ from a solvent of $\text{Li}_2\text{O}_3 \cdot 2\text{WO}_3$ plus 2.0% (by weight) B_2O_3 . The growth process was carried out in air at a temperature of approximately 1300 °C, and the resulting crystals were colorless octahedra with edge lengths up to 3.0 mm. Acrylic spray coatings were applied, and the crystals were sealed in cylindrical nylon capsules to prevent radioactive contamination.

Strontium chloride single crystals doped with $^{239}\text{Pu}^{3+}$ were grown by the vertical Bridgman technique according to the procedure described in Ref. 7. The $^{239}\text{Pu}^{3+}$ dopant was added to high-purity single-crystal fragments of SrCl_2 in the form of PuCl_3 , which was prepared by chlorinating PuO_2 with CCl_4 vapor at 800 °C.⁸ The resulting single crystals were colorless cylinders, ≈ 3.0 cm in length and about 0.5 cm in diameter. The tendency of SrCl_2 crystals to disintegrate in the presence of water vapor made application of an acrylic spray coating particularly important. Both of the crystal-growth procedures described above were carried out in a sealed system in order to contain the α -active dopants.⁹

The EPR spectra were observed at ≈ 9.0 GHz with

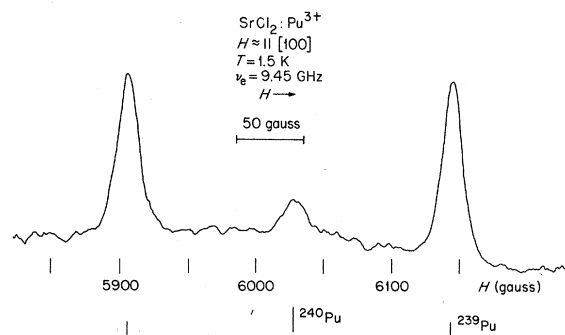


FIG. 1. EPR spectrum of $^{239}\text{Pu}^{3+}$ in SrCl_2 at 1.5 K with $\vec{H} \approx \parallel [100]$. (^{240}Pu is also present due to the decay of ^{244}Cm .)

both a superheterodyne spectrometer and a conventional homodyne spectrometer which used a back-diode detector. Since the resonance lines saturated easily, low-power operation was necessary with either spectrometer configuration. Both the ThO_2 and SrCl_2 crystals were mounted in the microwave cavity with a vertical $\langle 110 \rangle$ axis which was defined by the intersection of two $\{111\}$ faces. The crystals could be rotated *in situ* about a $\langle 111 \rangle$ axis which lay in the plane of rotation of the applied magnetic field. Precise magnetic-field-position measurements of electron-resonance lines were made by a simultaneous display of both the electron resonance and a nuclear-magnetic-resonance signal on a dual-beam oscilloscope.

III. RESONANCE RESULTS AND DISCUSSION

At 4.2 K the EPR spectrum of $^{239}\text{Pu}^{3+}$ in both ThO_2 and SrCl_2 consisted of two lines with isotropic magnetic-field positions and anisotropic linewidths. The narrowest linewidths occurred with the applied magnetic field oriented parallel to a $\langle 100 \rangle$ direction. Variation of the linewidth and apparent intensity as a function of magnetic-field orientation was such that the electron resonance could not be detected if the magnetic field was oriented in a general direction more than about 30° from a $\langle 100 \rangle$ axis. The spectrum of $^{239}\text{Pu}^{3+}$ in SrCl_2 at 1.5 K is shown in Fig. 1, where a weak third line located between the two stronger $^{239}\text{Pu}^{3+}$ hyperfine components can also be seen. This weak line is identified as a resonance transition of $^{240}\text{Pu}^{3+}$ which was present in small amounts in the dopant material. The resonance due to $^{240}\text{Pu}^{3+}$ was previously observed (but not identified) in single crystals of ThO_2 ¹⁰ and SrCl_2 ⁷ doped with $^{244}\text{Cm}^{3+}$. (The curium dopant had been separated for some time, and ^{240}Pu was present as a decay product of ^{244}Cm .) Although it is not apparent from Fig. 1, the high-field $^{239}\text{Pu}^{3+}$ line is slightly more intense and narrower than the low-field line and a similar variation could be detected for $^{239}\text{Pu}^{3+}$ in ThO_2 (Fig. 2).

The two-line spectrum of $^{239}\text{Pu}^{3+}$ is described by the spin Hamiltonian

$$\mathcal{H} = g\mu_B \vec{H} \cdot \vec{S} + A\vec{I} \cdot \vec{S}, \quad (1)$$

with $S = \frac{1}{2}$ and $I = \frac{1}{2}$. Values of the parameters g and A for $^{239}\text{Pu}^{3+}$ in ThO_2 and SrCl_2 are given in Table I along with the parameters obtained by Edelstein *et al.*¹ for $^{239}\text{Pu}^{3+}$ in CaF_2 , SrF_2 , and BaF_2 . The tabulated Pu^{3+} results are listed in order of decreasing crystal-field strength as suggested by the results on Gd^{3+} in these hosts.⁵ A general trend of decreasing g values and increasing A values with decreasing crystal-field strength is evident from the data presented in Table I. The different g values for Pu^{3+} in the alkaline-earth fluorides were accounted for by the equation¹

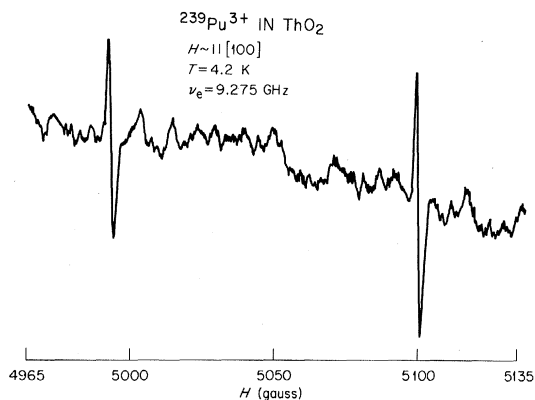


FIG. 2. EPR spectrum of $^{239}\text{Pu}^{3+}$ in ThO_2 at 4.2 K with $\vec{H} \approx \parallel [100]$.

$$g = -0.700 \cos^2 \phi + 3.254 \sin \phi + 2.595 \sin^2 \phi, \quad (2)$$

where ϕ is defined by the expression

$$|\Gamma_7^1\rangle = \cos \phi |J = \frac{5}{2}, \Gamma_7\rangle - \sin \phi |J = \frac{7}{2}, \Gamma_7'\rangle, \quad (3)$$

and therefore determines the degree of admixture of the Γ_7^1 doublet in the first excited $J = \frac{7}{2}$ state into the Γ_7 doublet in the ground $J = \frac{5}{2}$ state. The coefficients preceding the trigonometric functions in Eq. (2) were calculated by Edelstein *et al.*¹ using the complete intermediate-coupled wave functions. Values of ϕ corresponding to our measured g values for Pu^{3+} in ThO_2 and SrCl_2 are given in Table I.

The coefficients B_4' and $B_6'^{11}$ used to describe the crystal-field potential in tensor-operator form have been related to the angle ϕ in Ref. 1. Making the assumption that $B_6'/B_4' \approx -0.2$, we have determined rough values of B_4' for Pu^{3+} in ThO_2 and SrCl_2 using Fig. 2 of Ref. 1. These results are given in Table I along with the B_4' values obtained by Edelstein *et al.*¹ for the alkaline-earth fluorides. The ratio $B_6'/B_4' \approx -0.2$ holds for the lanthanide ions, and it was assumed in Ref. 1 that the same ratio would be valid for the actinide ions. The ordering of crystal-field strengths determined in this manner is consistent with that predicted by the point-charge model. Edelstein *et al.*¹ have noted, however, that the magnitude of the variation in crystal-field strengths is less than that predicted by the point-charge model for the three fluoride hosts. Our results for Pu^{3+} in ThO_2 and SrCl_2 are consistent with their observation.¹²

Edelstein and Mehlhorn⁴ have interpreted their measurements of the $^{239}\text{Pu}^{3+}$ hyperfine parameters in the fluorides by writing the hyperfine constant A as the sum of two components, A_f and A_c , where

$$A_f = \theta \langle \Gamma_7^1 | \sum_i \vec{N}_i | \Gamma_7^1 \rangle \quad (4)$$

and

$$A_c = C \langle \Gamma_7^1 | \sum_i \vec{s}_i | \Gamma_7^1 \rangle \quad (5)$$

where

$$\vec{N}_i = \vec{l}_i - \vec{s}_i + 3\vec{r}_i (\vec{s}_i \cdot \vec{r}_i) / r_i^2 \quad (6)$$

and \vec{l}_i and \vec{s}_i are, respectively, the orbital and spin angular-momentum vectors and \vec{r}_i is the radius vector of the i th electron.

The coefficient θ in Eq. (4) is given by the expression

$$\theta = (4\mu_B\mu_N\mu_I/I) \langle r^{-3} \rangle, \quad (7)$$

where μ_B and μ_N are the Bohr magneton and nuclear magneton, respectively, and μ_I is the magnetic moment in units of nuclear magnetons.

The coefficient C in Eq. (5) is proportional to μ_I/I and represents the effects of a contact interaction due to core polarization. (Relativistic contributions can also affect the value of C .) The matrix elements in Eqs. (4) and (5) can be evaluated using the tables given in Ref. 4 and the appropriate values of ϕ . The two equations in θ and C resulting from the values of ϕ for $^{239}\text{Pu}^{3+}$ in ThO_2 and SrCl_2 plus the three equations⁴ obtained for Pu^{3+} in the fluorides are given by

$$\text{ThO}_2: A = -0.599\theta - 0.001C = -65.38 \times 10^{-4} \text{ cm}^{-1},$$

$$\text{CaF}_2: A = -0.644\theta + 0.028C = -67.2 \times 10^{-4} \text{ cm}^{-1},$$

$$\text{SrF}_2: A = -0.733\theta + 0.086C = -84.6 \times 10^{-4} \text{ cm}^{-1},$$

$$\text{BaF}_2: A = -0.832\theta + 0.154C = -102 \times 10^{-4} \text{ cm}^{-1},$$

$$\text{SrCl}_2: A = -0.918\theta + 0.216C = -127.9 \times 10^{-4} \text{ cm}^{-1}. \quad (8)$$

Edelstein and Mehlhorn have calculated values of $98.1 \times 10^{-4} \text{ cm}^{-1}$ for θ and $-147 \times 10^{-4} \text{ cm}^{-1}$ for C from the equations obtained with their fluoride A values. We obtain the best fit (weighted least squares) to all five equations with values of 105.2

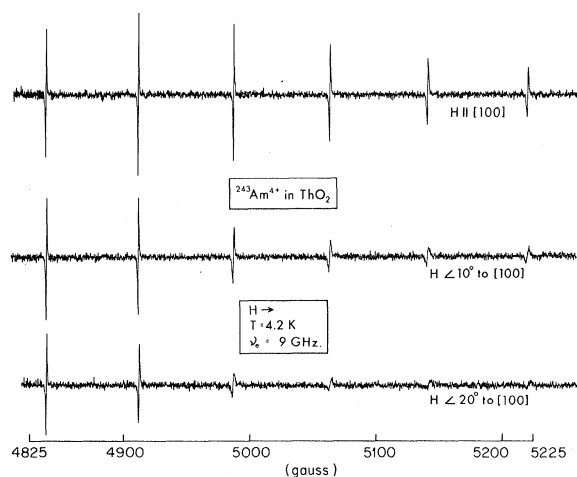


FIG. 3. EPR spectra of $^{243}\text{Am}^{4+}$ in ThO_2 at 4.2 K. In the top trace, $\vec{H} \parallel [100]$, while for the middle and bottom traces, \vec{H} is at angles 10° and 20° to $[100]$, respectively.

TABLE I. Spin-Hamiltonian parameters for $5f^5$ configuration ions.

Ion	Matrix	$ g $	$ A $ (10^{-4} cm $^{-1}$)	ϕ (deg)	$B_4'^a$ (cm $^{-1}$)	Ref.
$^{239}\text{Pu}^{3+}$	ThO $_2$	1.3124 \pm 0.0005	65.4 \pm 0.2	-16.0	-6600	b
$^{239}\text{Pu}^{3+}$	CaF $_2$	1.297 \pm 0.002	67.2 \pm 0.6	-15.1	-6200	c
$^{239}\text{Pu}^{3+}$	SrF $_2$	1.250 \pm 0.002	84.6 \pm 1.0	-13.2	-5400	c
$^{239}\text{Pu}^{3+}$	BaF $_2$	1.187 \pm 0.004	102 \pm 3	-11.0	-4600	c
$^{239}\text{Pu}^{3+}$	SrCl $_2$	1.1208 \pm 0.0005	127.9 \pm 0.4	-9.0	-4000	b
$^{241}\text{Am}^{4+}$	ThO $_2$	1.2862 \pm 0.0005	45.7 \pm 0.1	b
$^{243}\text{Am}^{4+}$	ThO $_2$	1.2862 \pm 0.0005	45.3 \pm 0.1	b

^aValues of B_4' were calculated assuming that $B_6'/B_4' = -0.2$.

^bThis work.

^cReference 1.

$\times 10^{-4}$ cm $^{-1}$ for θ and -131.5×10^{-4} cm $^{-1}$ for C . These values of θ and C fit the five measured A values to within $\approx 6.0\%$. (The worst fit is obtained for $^{239}\text{Pu}^{3+}$ in BaF $_2$, a system for which Edelstein *et al.*¹ obtained their least reliable data. Disregarding the A value quoted for BaF $_2$, our values of θ and C fit the remaining four experimentally determined A values to within $\approx 4.0\%$.) From the parameter C , an expression for the core-polarization hyperfine term for the free-ion pure J ground state may be written

$$a_c = -(492 \pm 50)(g_J - 1)\mu_I/I \text{ MHz.} \quad (9)$$

From θ , using Eq. (7), the $\text{Pu}^{3+} \langle 1/r^3 \rangle$ value is computed to be 4.13 ± 0.33 a. u.

The EPR spectra of $^{241}\text{Am}^{4+}$ and $^{243}\text{Am}^{4+}$ in ThO $_2$ were observed at 4.2 K. The spectrum of each isotope consisted of six lines with isotropic magnetic-field positions and anisotropic linewidths. Line-width variations with applied magnetic-field orientation were similar to those observed for Pu^{3+} , and Am^{4+} linewidths were narrowest for $H \parallel \langle 100 \rangle$. A strong dependence of both the linewidth and integrated intensity on the nuclear-spin-projection quantum number m_I was observed, and this effect is illustrated by the top trace in Fig. 3. Rotation of the magnetic field away from a $\langle 100 \rangle$ direction enhanced the differences in linewidth and intensity between the m_I components as illustrated by the lower two traces in Fig. 3. The spectrum observed for each americium isotope was described by the spin Hamiltonian given in Eq. (1) with $S = \frac{1}{2}$ and $I = \frac{5}{2}$. Table I lists the resulting g and A values. The ratio $^{241}\text{A}/^{243}\text{A} = 1.009$ is in agreement with the re-

sult obtained previously for Am^{2+} in SrCl $_2$ ⁷ and CaF $_2$.¹³ Unfortunately the intermediate-coupled wave functions are not available for Am^{4+} , and an analysis similar to that carried out for Pu^{3+} is not possible at this time.

IV. CONCLUSION

The EPR results for $^{239}\text{Pu}^{3+}$ in ThO $_2$ and SrCl $_2$ show that the analysis and interpretations of Edelstein *et al.*^{1,4} can account for the observed g and A values over a wide range of crystal-field strengths. Rough calculations of B_4' , a fourth-order crystal-field parameter, yielded results which were consistent with previously observed variations in crystal-field strength. The significant variations in intensity and linewidth as a function of applied field orientation and the variation with m_I are not presently understood, but are currently the subject of an extended investigation.

Note added in proof. There is an error of a factor of 2 in the conversion of θ to $\langle 1/r^3 \rangle$ in Ref. 4 which would change their value to 3.85 a. u. [N. Edelstein (private communication).] We are unable to explain the discrepancy between these experimental values for $\langle 1/r^3 \rangle$ and the larger values calculated by W. Burton Lewis, Joseph B. Mann, David A. Liberman, and Don T. Cromer [J. Chem. Phys. **53**, 809 (1970)].

ACKNOWLEDGMENTS

The authors gratefully acknowledge helpful discussions with N. Edelstein and the cooperation of O. L. Keller and the staff members of the ORNL Transuranium Research Laboratory.

[†]Research sponsored by the U. S. Atomic Energy Commission under contract with Union Carbide Corp.

*Advanced Technology Center, Inc. (formerly LTV Research Center), Dallas, Tex.

[‡]Metals and Ceramics Division, Oak Ridge National Laboratory, Oak Ridge, Tenn.

¹N. Edelstein, H. F. Mollet, W. C. Easley, and R. J. Mehlhorn, J. Chem. Phys. **51**, 3281 (1969). The calculation of intermediate-coupled wave functions re-

ported in this reference was based on the optically derived spin-orbit and electrostatic parameters of Sm^{3+} [W. T. Carnall, P. R. Fields, and K. Rajnak, *ibid.* **49**, 4424 (1968)] and Pu^{3+} [J. G. Conway and K. Rajnak, *ibid.* **44**, 348 (1966)].

²W. Low, Phys. Rev. **134**, A1479 (1964).

³A. A. Antipin, I. N. Kurkin, L. D. Livanova, I. Z. Potvorova, and L. Ta. Shekun, Fiz. Tverd. Tela **7**, 1575 (1965) [Sov. Phys. Solid State **7**, 1271 (1965)].

⁴N. Edelstein and R. Mehlhorn, Phys. Rev. B 2, 1225 (1970).

⁵M. M. Abraham and L. A. Boatner, J. Chem. Phys. 51, 3134 (1969).

⁶C. B. Finch and G. W. Clark, J. Appl. Phys. 36, 2143 (1965).

⁷M. M. Abraham, L. A. Boatner, C. B. Finch, R. W. Reynolds, and H. Zeldes, Phys. Rev. B 1, 3555 (1970).

⁸B. M. Abraham, B. B. Brody, N. R. Davidson, F. Hageman, I. Karle, J. J. Katz, and M. J. Wolf, in *Transuranium Elements*, edited by G. T. Seaborg, J. J. Katz, and W. M. Manning (McGraw-Hill, New York, 1949), p. 740.

⁹Crystal-growth procedures were accomplished using the containment facilities of the ORNL Transuranium Research Laboratory.

¹⁰M. M. Abraham, C. B. Finch, and G. W. Clark, Phys. Rev. 168, 933 (1968).

¹¹B. G. Wybourne, *Spectroscopic Properties of Rare*

Earths (Interscience, New York, 1965). The coefficients B'_4 and B'_6 of the tensor operators are given by $B'_4 = 8B_4/\beta$ and $B'_6 = 16B_6/\gamma$, where B_4 and B_6 are the spin-Hamiltonian parameters, and β and γ are Stevens's operator equivalents as used by K. R. Lea, M. J. M. Leask, and W. P. Wolf, J. Phys. Chem. Solids 23, 1381 (1962).

¹²For each host, two values of ϕ result from a solution of Eq. (2). The angle which is larger in absolute value is disregarded since it leads to an incorrect ordering of crystal-field strengths in every case except ThO₂. For the latter, there remains the possibility that the larger angle may still be appropriate. The larger value of $\phi = -28.6^\circ$ for ThO₂ implies a value of the crystal-field parameter B'_4 which is approximately twice that found for CaF₂ (with the assumption that $B'_6/B'_4 = -0.2$) and is inconsistent with previous determinations of relative crystal-field strengths for these two hosts.

¹³N. Edelstein, W. Easley, and R. McLaughlin, J. Chem. Phys. 44, 3130 (1966).

Nuclear Spin Diffusion Induced by Paramagnetic Impurities in Nonconducting Solids*

E. Philip Horvitz[†]

Rice University, Houston, Texas 77001

(Received 13 February 1970)

It is shown that paramagnetic impurities can induce nuclear spin diffusion in nonconducting solids. The component of the impurity spin along the external magnetic field (assumed to be the z axis), because of its interaction with the lattice, fluctuates. The resulting spectral intensity of the magnetic moment has components at all frequencies. The component at zero frequency creates a static magnetic field which is different at two neighboring nuclei, thereby splitting the levels $|\frac{1}{2}, -\frac{1}{2}\rangle$ and $|\frac{1}{2}, \frac{1}{2}\rangle$, where the first and second quantum numbers refer, respectively, to the z components of two neighboring spins. These are exact two-spin eigenfunctions if the interaction of the nuclear spins is neglected. When this is taken into account, the correct eigenfunctions to first order are $\psi_1 = |\frac{1}{2}, -\frac{1}{2}\rangle + \epsilon |\frac{1}{2}, \frac{1}{2}\rangle$ and $\psi_2 = |\frac{1}{2}, \frac{1}{2}\rangle - \epsilon |\frac{1}{2}, -\frac{1}{2}\rangle$, where ϵ is a small number. The Fourier component of the impurity spin at the frequency corresponding to the energy difference of ψ_1 and ψ_2 causes transitions between these states. This is a spin-diffusion process because ϵ is small. This means that Bloembergen's differential equation for nuclear spin-lattice relaxation in nonconducting solids must be generalized to include nuclear spin diffusion inside the critical radius.

I. INTRODUCTION

Bloembergen¹ first showed the importance of paramagnetic impurities in nuclear spin-lattice relaxation in nonconducting solids. His theory states that nuclear relaxation is the result of two mechanisms. One is the direct relaxation of nuclei by paramagnetic impurities and the other is nuclear spin diffusion,² which arises from the nuclear dipole-dipole interaction and is on the order of 10^{-12} cm²/sec.

The spins closest to the impurity feel the greatest direct relaxation rates and this creates a gradient in the magnetization. Spin diffusion transports the magnetization throughout the sample, thereby

smoothing out the gradient and increasing the relaxation rate. Bloembergen set up the differential equation that describes this relaxation process:

$$\frac{\partial m}{\partial t} = D\nabla^2 m - \frac{C}{r^6} m. \quad (1)$$

m is the difference between the instantaneous value of the magnetization and the equilibrium value of the magnetization, D is the nuclear-spin-diffusion coefficient, r is the distance of the nuclear spins from the paramagnetic impurity, and C is a coefficient that describes the effect of direct relaxation. He introduced the boundary condition that spin diffusion vanishes inside a critical radius r_c . This radius is where the static field of the impurity spin splits ad-